Antiscreening mode of projectile-electron loss

C. C. Montanari,[1,2] J. E. Miraglia,[1,2] and N. R. Arista[3]
[1]*Instituto de Astronomía y Física del Espacio, Casilla de Correo 67, Sucursal 28, 1428 Buenos Aires, Argentina*
[2]*Facultad de Ciencias Exactas y Naturales, Universidad de Buenos Aires, Buenos Aires, Argentina*
[3]*Instituto Balseiro, Centro Atomico Bariloche, 8400 Bariloche, Argentina*
(Received 6 January 2003; published 5 June 2003)

The inelastic contribution of target electrons to different electronic processes in the projectile is obtained by employing the local-density approximation as usually applied in the dielectric formalism. Projectile-electron-loss cross sections due to the electron-electron interaction are calculated and compared with those obtained by using atomic antiscreening theories. We also calculate ionization cross sections and stopping power for bare ions impinging on different gases. The good agreement with the experimental data and the simplicity of the local-density approximation make it an efficient method for describing inelastic processes of gaseous target electrons. It is expected to be useful for targets with large atomic number. In this case, the number of possible final states to be considered by the traditional atomic methods makes it a tough task to be tackled. On the contrary, the more electrons the target has, the better the local plasma approximation is expected to be.

DOI: 10.1103/PhysRevA.67.062702 PACS number(s): 34.50.Fa

I. INTRODUCTION

Ion-atom collisions including inelastic processes in the target and the projectile electrons have received considerable attention in recent years [1–4]. In general, projectile-electron transitions occur via interaction with the screened target nucleus (target electrons frozen in their initial state) and via the electron-electron interaction (target electrons playing an active role and being excited). These modes of interactions are known as screening and antiscreening modes, respectively [5,6]. From the work of McGuire, Stolterfoht, and Simony [5] 20 years ago, up to recent calculations of Kirchner and Horbatsch [4], the antiscreening contribution to different processes in the projectile has been an object of many studies [1–3,6–15]. The main problem of having a complete antiscreening picture is the description of the whole set of final states. Some approximations were developed that make use of the closure relation for the final states of the target electrons [5,7,8].

The purpose of this work is to present an alternative way of considering the antiscreening contribution by describing the whole set of target electrons employing the dielectric formalism. The goal of this model is the simplicity of the description, and fast calculation as compared with the usual antiscreening calculations [4–8].

The employment of the dielectric formalism followed here to describe gaseous targets lay upon two previous works. One in which the physical pictures represented by the dielectric and the binary collision formalisms are compared [16,17]. The other one is a recent work [18] in which we consider the bound electrons of solids by using the local plasma approximation (LPA) [19–22]. This model considers that under certain conditions (fast heavy projectiles, high impact velocities as compared to those of the electrons in the shells), bound electrons react to the ion perturbation as free electrons. In this way, they are approximated as a free-electron gas of inhomogeneous density which is polarized by the ion pass. The excitation of this free-electron gas is described as a whole by employing the known dielectric formalism [23,24]. In the case of projectile inelastic processes, such as electron loss, the LPA allows us to evaluate the simultaneous excitation of projectile and target bound electrons. This is the antiscreening mode.

In this contribution, we employ the LPA to deal with the bound electrons of gas targets in a way analogous to that used to deal with solid bound electrons [18]. A study of the validity of the model in the test system proton hydrogen has already been published by Sarasola *et al.* [22].

The work is organized as follows. In Sec. II, we briefly summarize the theoretical model employed, and present a link with the usual antiscreening calculations. In Sec. III we present the results of employing the LPA in antiscreening calculations of projectile-electron loss cross sections. We also present in Sec. III the results of employing the model in dealing with the collisions of bare ions with gases. This allows us to isolate the LPA description of target electrons and check it with the large variety of experimental data available of ionization cross sections and stopping power. Finally, the conclusions are left to Sec. IV. Atomic units are used throughout this work.

II. THEORY

A. The local plasma approximation

We consider the collisions of hydrogenic projectiles of nuclear charge Z_P and velocity v with the electrons of neutral targets. The LPA [20] considers that target electrons react to the external perturbation as free particles. They are described at each point of the space as a free-electron gas of space-dependent density $n(r)$. In the present version of the LPA, the density of bound electrons is obtained from the atomic Hartree-Fock wave functions [25]. It lets us to consider either each shell separately or the whole set of bound electrons by adding the shell densities [18].

Probabilities per unit length for projectile-electron excitation or loss are obtained by employing the dielectric formalism in a way analogous to that related to projectiles interacting with the free-electron gas of metals [23]. The difference

is centered in the space-dependent density of the target bound electrons. The link between these probabilities and the binary collision ones can be found in Ref. [16].

For projectile-electron excitation from an initial state i to an excited state f, the probability per unit length reads [16]

$$P_{if}=\frac{2}{\pi v^2}\int_{q_0}^{\infty}\frac{dq}{q}\int_0^{qv-\Delta\epsilon}|F_{if}(q)|^2\mathrm{Im}\left[-\frac{1}{\varepsilon(q,\omega)}\right]d\omega, \tag{1}$$

where $q_0=\Delta\epsilon/v$ is the minimum momentum transferred, $\Delta\epsilon$ is the energy gained by the projectile electron, $\varepsilon(q,\omega)$ is the dielectric function, and

$$F_{if}(q)=\langle\psi_f|e^{i\vec{q}\cdot\vec{r}}|\psi_i\rangle \tag{2}$$

is the projectile form factor considering unperturbed initial and final wave functions (first Born approximation). The variables q and ω represent the momentum transfer and the energy gained by the target electrons.

The LPA [20] assumes bound electrons as a gas of free electrons of density $n(R)$, then the dielectric function $\varepsilon^{LPA}(q,\omega)$ is related to the known Linhard dielectric response of the free-electron gas, $\varepsilon(q,\omega,n(R))$, by

$$\mathrm{Im}\left[\frac{-1}{\varepsilon^{LPA}(q,\omega)}\right]=n_T\int d\vec{R}\,\mathrm{Im}\left[\frac{-1}{\varepsilon(q,\omega,n(R))}\right], \tag{3}$$

with n_T being the density of target atoms.

For solid targets, this density is fixed and the space mean value in the dielectric function is obtained by integrating up to the radius of the Wigner-Seitz cell, $R_{WS}=[3/(4\pi n_T)]^{1/3}$. For gaseous targets, the spatial integration is extended over the whole space, and it is convergent because $n(R)$ tends to zero drastically for large R.

The cross section per atom for projectile-electron excitation in the LPA is given by

$$\sigma_{if}^{LPA}=\frac{P_{if}}{n_T}=\frac{2}{\pi v^2}\int_{q_0}^{\infty}\frac{dq}{q}|F_{if}(q)|^2 g_0^{LPA}(q), \tag{4}$$

with

$$g_n^{LPA}(q)=\int_0^{qv-\Delta\epsilon}\omega^n\,d\omega\int d\vec{R}\,\mathrm{Im}\left[-\frac{1}{\varepsilon(q,\omega,n(R))}\right]. \tag{5}$$

The cross section expressed in Eq. (4) is independent of the density of target atoms as it is expected. The generalized function $g_n^{LPA}(q)$ allows us to express the energy moments; i.e., the stopping power $(n=1)$ can be written as

$$S_{if}^{LPA}=\frac{2}{\pi v^2}\int_{q_0}^{\infty}\frac{dq}{q}|F_{if}(q)|^2 g_1^{LPA}(q). \tag{6}$$

In the case of projectile-electron loss, the energy gained by the projectile electron is $\Delta\epsilon=k^2/2-\epsilon_i$, with $\vec{k}$ being the momentum of the ionized electron. Then the total cross sections are obtained from Eq. (4) with an additional integration in the $\vec{k}$ space. The projectile ionization form factor is calculated in the first Born approximation in the usual way [26–30], with the loss electron described by the Coulomb wave function in the continuum of the projectile.

On the other hand, if we are interested in the collisions of bare projectiles with neutral atoms, we must consider the nucleus-electron interaction instead of the electron-electron one. In this case, the cross section and stopping power can be obtained from Eqs. (4) and (6) by replacing $\Delta\epsilon$ by 0 and the projectile form factor $|F_{if}(q)|^2$ by Z_P^2.

The LPA considers a free-electron gas of local density $n(R)$ and an initial momentum distribution $k_i\leqslant k_F(R)=[3\pi^2 n(R)]^{1/3}$. The dielectric function assumes final states different from the initial ones, i.e., $k_f>k_F(R)$. It means that by employing this formalism, we obtain the probabilities of projectile-electron excitation or loss due to collisions with the target electrons that do change of state. Moreover, we are considering the whole picture of final states of the target electrons different from the initial one. This is the whole antiscreening contribution.

The LPA proposed here makes use of the Linhard dielectric response [31]. It implies that it does not describe the electrons just as independent particles. Instead, bound electrons are considered as a local free-electron gas which incorporates the electron-electron interaction to all orders. The energy conservation is relaxed following the dielectric formalism that allows collective excitations of the electrons together with the single-electron ones included in the binary collision formalism [16,17,24].

If we consider the single-particle approximation of the dielectric function, we can compare the bound-electron response given by the LPA with that of actually free electrons. The single-particle dielectric function ε^{SP} [23] reads

$$\mathrm{Im}\left[-\frac{1}{\varepsilon^{SP}(q,\omega,R)}\right]=\frac{4\pi^2}{q^2}n(R)\,\delta(\omega-q^2/2). \tag{7}$$

The space integration of this dielectric function following Eq. (3) so as to get ε^{LPA} gives

$$\int d\vec{R}\,\mathrm{Im}\left[-\frac{1}{\varepsilon^{SP}(q,\omega,R)}\right]=\frac{4\pi^2}{q^2}N_e\,\delta(\omega-q^2/2), \tag{8}$$

where $N_e=\int d\vec{R}\,n(R)=Z_T$ is the number of target electrons. Then the LPA cross section given by Eq. (4) calculated in the single particle approximation reads

$$\sigma_{SP}^{LPA}=\frac{8\,N_e}{v^2}\int_{q_0}^{\infty}|F_{if}(q)|^2\frac{dq}{q^3}=N_e\sigma^e, \tag{9}$$

which is just the excitation cross section by N_e electrons. When the δ function of Eq. (8) is introduced in Eq. (4), it gives null result if $qv<\Delta\varepsilon+q^2/2$, i.e., a projectile impact energy less than the energy gained by the free electron plus the excitation energy of the projectile electron.

The complete LPA cross sections will be always lower than this free-electron value, $\sigma^{LPA}=N_e'\sigma^e$, with $N_e'<N_e=Z_T$, due to the shielding of the ion potential by the target electrons, as described in a previous work [16]. This behavior is similar to that recently pointed out by Montenegro *et al.* [32].

B. Comparison with the atomic antiscreening theories

As already mentioned, the main problem of the traditional atomic methods to have a complete antiscreening picture is the description of the whole set of final states of the target electrons. Some approximations were developed that make use of the closure relation for the final states of the target electrons [5–7,12]. The employment of the closure relation is possible when the minimum momentum transferred q_n can be approximated by a fixed value independent of the target electron final state n. For instance, the approximation of McGuire, Stolterfoht, and Simony [5] considers $q_n \simeq q_0$, the minimum momentum transferred due to the energy gained by the projectile electron. Instead, the antiscreening approximation introduced by Montenegro and Meyerhof [7] proposes a mean value of the minimum momentum transferred, related to Bethe's sum rule $\overline{q}=q_0+\delta$. Thus, for the most asymmetric systems and high velocity conditions $\delta \ll q_0$ and the first approximation is reobtained.

The complete antiscreening cross section [7] is

$$\sigma_{if}^{ant}=\frac{8\pi}{v^2}\sum_{m\neq 0}\int_{q_0+q_m}^{\infty}\frac{dq}{q^3}|F_{if}(q)|^2\left|\langle\chi_m|\sum_j e^{i\vec{q}\cdot\vec{r}j}|\chi_0\rangle\right|^2, \tag{10}$$

with $F_{if}(q)$ being the projectile form factor, χ_0 and χ_m being the initial and final states of the target electrons, E_0 and E_m the corresponding energies and the momentum transferred $q_m=(E_m-E_0)/v$. If we introduce the energy gained by the target electron as a new variable ω, Eq. (10) can be rewritten as

$$\sigma_{if}^{ant}=\frac{8\pi}{v^2}\sum_{m\neq 0}\int_0^{\infty}\delta(\omega-E_m+E_0)d\omega \times\int_{q+\omega/v}^{\infty}\frac{dq}{q^3}|F_{if}(q)|^2\left|\langle\chi_m|\sum_j e^{i\vec{q}\cdot\vec{r}_j}|\chi_0\rangle\right|^2. \tag{11}$$

A change of the order of the integrals gives

$$\sigma_{if}^{ant}=\frac{2}{\pi v^2}\int_{q_0}^{\infty}\frac{dq}{q}|F_{if}(q)|^2 g^{ant}(q) \tag{12}$$

with

$$g^{ant}(q)=\frac{4\pi^2}{q^2}\sum_{m\neq 0}\int_0^{qv-\Delta\epsilon}d\omega\,\delta(\omega-E_m+E_0)\times\left|\langle\chi_m|\sum_i e^{i\vec{q}\cdot\vec{r}_i}|\chi_0\rangle\right|^2. \tag{13}$$

In this way we write the atomic antiscreening cross section σ_{if}^{ant} in a shape analogous to that of σ_{if}^{LPA} given by Eq. (4). The δ function in Eq. (13) implies that $g^{ant}(q)=0$ if $qv<\Delta\varepsilon+E_m-E_0$. It means that it explicitly has the threshold for the electron-loss process signed by Anholt [6] as one defect of the closure approximation.

The antiscreening cross section given by Eq. (12) can be written in terms of a dielectric response of the medium so that

$$\sigma_{if}^{ant}=\frac{2}{\pi v^2}\int_{q_0}^{\infty}\frac{dq}{q}|F_{if}(q)|^2\int_0^{qv-\Delta\epsilon}d\omega\,\mathrm{Im}\left[\frac{-1}{\varepsilon^{ant}(q,\omega)}\right], \tag{14}$$

with $\varepsilon^{ant}(q,\omega)$ given by

$$\mathrm{Im}\left[\frac{-1}{\varepsilon^{ant}(q,\omega)}\right]=\frac{4\pi^2}{q^2}\sum_{m\neq 0}\delta(\omega-E_m+E_0)\times\left|\langle\chi_m\sum_i e^{i\vec{q}\cdot\vec{r}_i}|\chi_0\rangle\right|^2. \tag{15}$$

This expression condenses all the inelastic processes of the target electrons allowed in a binary collision. The comparison between the atomic and dielectric descriptions is then reduced to compare the response functions $\varepsilon^{ant}(q,\omega)$ and $\varepsilon^{LPA}(q,\omega)$. In fact, these functions represent the physical picture given by each formalism (atomic and dielectric) for the response of the target electrons to the projectile perturbation.

III. RESULTS

We describe the target bound electrons by using the corresponding Hartree-Fock [25] wave functions, and the space-dependent densities for each level obtained from them. These densities are included in the Linhard dielectric response, which is space averaged to give the LPA dielectric function ε^{LPA} of Eq. (3). In what follows we have employed the LPA for the collisions of bare and dressed ions with noble gases.

A. Collisions with bare projectiles

In order to isolate the LPA description of gas target response, we analyze first the collisions with bare ions. This gives us the possibility of a direct comparison with the experimental data of proton-gases collisions. One particular magnitude to inspect is the ionization cross section. As mentioned before, the LPA describes the response of the electronic system as a whole. It gives the contribution from any possible final excited state of the target electrons. However, the LPA as presented here, allows us to evaluate the contribution of each shell separately. In the case of ionization, we do know the final state. We must consider those final states that imply a jump in the electron energy higher than the ionization threshold of each shell, ϵ_n. This fact is introduced by integrating Eq. (4) in the energy gained by the electrons so that $\omega>\epsilon_n$. The ionization thresholds are given by the Hartree-Fock [25] energies of each level. This method has

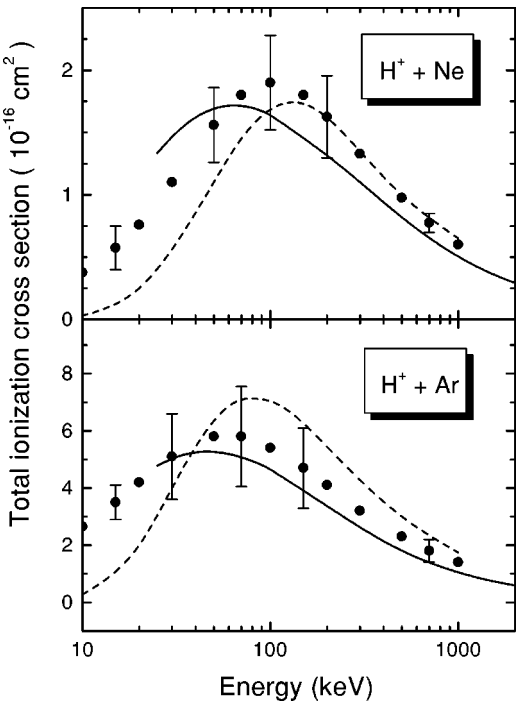

FIG. 1. Ionization cross sections of Ne and Ar by proton impact, as functions of the projectile energy. Notation: solid lines, our LPA results; dashed lines, CDW-EIS calculations [34]; filled circles, experimental data of Rudd *et al.* [35].

already been applied to inner-shell ionization of solid atoms with very good accord with the experimental data [18,33].

Figure 1 shows the LPA total cross sections for the ionization of Ne and Ar by H^+ impact. The LPA results are displayed together with the continuum distorted wave-eikonal initial-state (CDW-EIS) curves [34] and with experimental data [35]. The agreement with the experimental measurements and with the CDW-EIS is very good, especially for impact energies above that of the maximum cross section.

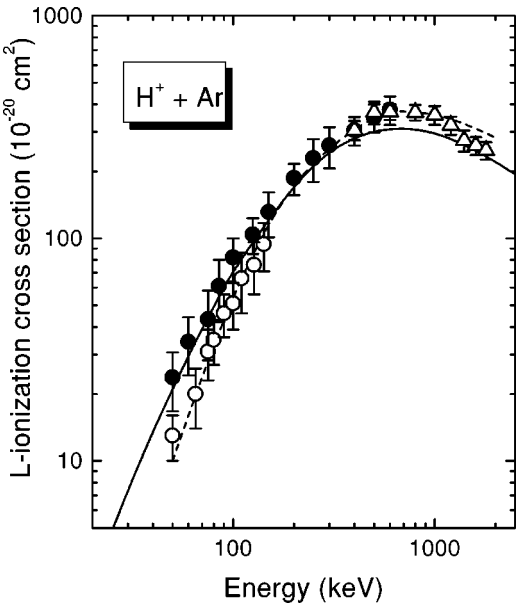

FIG. 2. *L*-shell ionization cross sections of Ar by proton impact. Notation: solid lines, our LPA results; dashed lines, CDW-EIS calculations [34]; experiments, open circles, Rudd [37]; closed circles, Stolterfoht *et al.* [36]; open triangles, Ariyasinghe *et al.* [38].

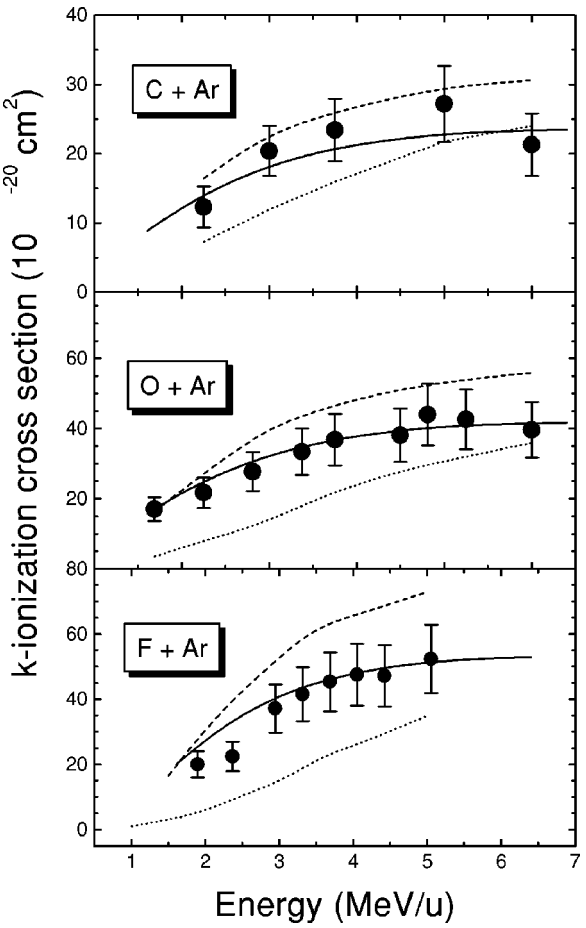

FIG. 3. *K*-shell ionization cross sections of Ar by interacion of different ions. Notation: solid lines, our LPA results; dotted lines, CDW-EIS calculations [39]; dashed lines, the perturbed stationary-state (ECPSSR) model [39]; experimental data of Dhal *et al.* [39].

The LPA is expected to be valid when the cloud of target electrons can be described as a free-electron gas. This condition can be expressed in terms of the impact velocity as $v > v_e$ (impact velocity higher than the target electron velocity). If we consider $v > Z_T$, this condition is fulfilled by all target electrons. However, in Fig. 1 we find very good accord with the experimental data even for velocities much lower than this. This behavior is explained by considering the velocities of the electrons shell by shell. The condition $v > v_e$ can be valid for the electrons of the outer shells, less bound and not for those of the inner shells. In the case of Ar, the main contribution to the total ionization cross sections comes from the $3p$ electrons (binding energy $\epsilon_{3p} = -0.59$ a.u. and $v_{3p} \approx 1.2$ a.u) [25]. They are liable to be approximated as free electrons for impact energies $E > 30$ keV. In an analogous way, the LPA is expected to be good for the ionization of Ne by protons at impact energies $E > 45$ keV. These results are in good accord with the performance of the LPA displayed in Fig. 1.

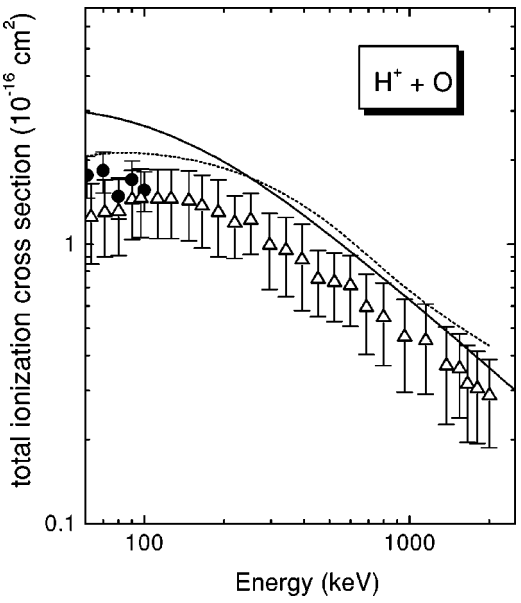

FIG. 4. Total ionization cross sections of O by proton impact. Notation: solid lines, our LPA results; dotted line, basis generator method of Kirchner *et al.* [40]; experimental data of Thompson *et al.* for *p*-O collisions [42], full circles; and for *e*-O collisions [43], hollow triangles.

The same range of validity can be observed in Fig. 2. In this case we display the LPA cross sections considering only the ionization of the *L* shell of Ar. Again the agreement with the experimental data and with the CDW-EIS calculation [34] is very good.

In Fig. 3, we compare the LPA results with recent measurements of the *K*-shell ionization of Ar by different projectiles made by Dhal *et al.* [39]. Figure 3 shows the LPA curve together with the experimental results and other theoretical

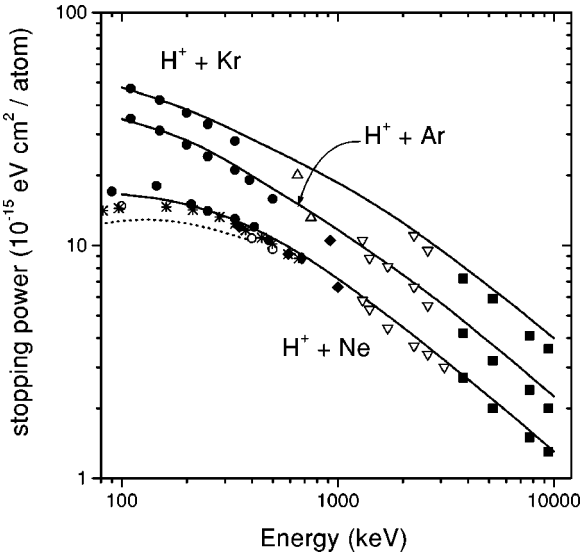

FIG. 5. Stopping power per atom in the collisions of protons on several gases. Notation: solid line, our LPA calculations; dotted line, END model results [46]; experimental data, hollow circles [47], stars [48], and from Refs. [44] and [45].

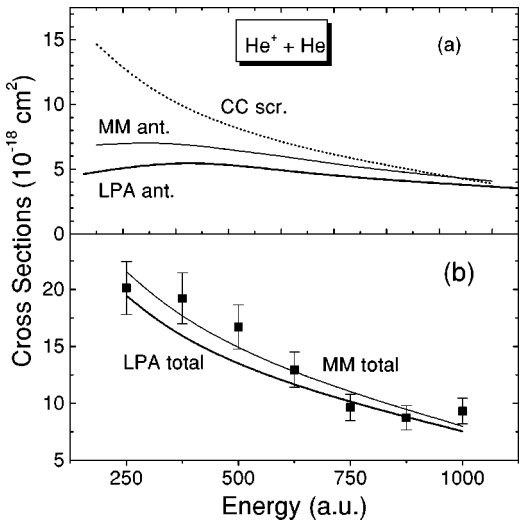

FIG. 6. Projectile-electron-loss cross sections as functions of the impact energy for He^+ impinging on He. Notation: (a) thick solid line, present LPA results; thin solid line antiscreening calculations following the procedure of Montenegro and Meyerhof [1,7]; dotted line, Grande *et al.* screening curve [1]; (b) solid line, the total electron-loss cross sections obtained by adding the LPA antiscreening contribution and the Grande *et al.* screening one; squares, measurements of Sant'Anna *et al.* [50].

calculations. It must be said that the employment of the LPA in this case means exploring the borders of the validity of the model, i.e., only two electrons and in the hardly bound state.

We also compare our results with the high-energy limit of the basis generator method, developed by Kirchner *et al.* [40,41]. This is a nonperturbative method that extends to a much larger energy range. In Fig. 4, we display the total ionization of O by proton impact. The impact energies shown correspond to impact velocities higher than those of the *L*-shell electrons of O. The agreement between both theoretical curves is very good, even when the LPA tends to overestimate the data for the lowest energies considered. Similar results are found for the total ionization of Ne by He^{2+} at energies greater than 200 keV [44].

Finally, stopping-power results for protons and α particles impinging on different gases are displayed in Fig. 5. Together with the experimental data available, we partially include the theoretical curve of Cabrera-Trujillo *et al.* [46] employing the electron-nuclear dynamics (END) model. Again, the LPA stands as a good high-energy description, but it cannot describe low-energy effects such as the threshold effect mentioned by these authors [46].

Figures 1–5 show that the LPA gives a good description of the atomic processes that take place in gaseous targets.

B. Electron-loss processes in hydrogenic projectiles

By employing the mentioned LPA, we obtained the antiscreening contribution to the electron-loss cross sections of He^+ ions impinging upon He, Ne, Ar, and Kr. The screening contribution is not included in the LPA calculations, since it considers only the inelastic processes of the target electrons.

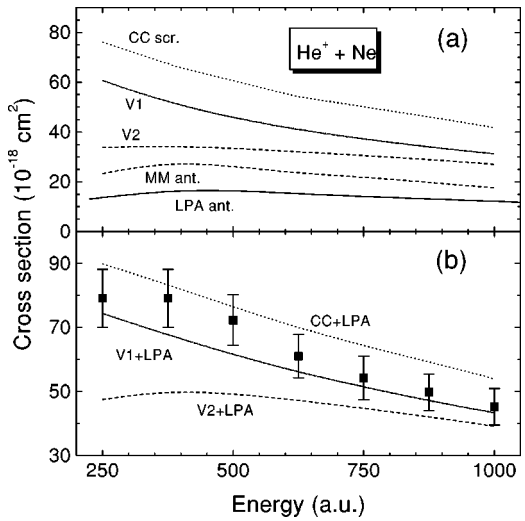

FIG. 7. Projectile-electron-loss cross sections for He^+ impinging on Ne. Notation: (a) thick solid line, presents LPA results; thin solid line, antiscreening calculations following the procedure of Montenegro and Meyerhof [3,7]; dotted line, Grande *et al.* screening curve [1]; dash-dotted line, nonperturbative screening of Voitkiv *et al.* [49]; dashed line, Voitkiv *et al.* screening calculation corrected by considering the probability of target electron ionization [3]; (b) theoretical curves of the total electron-loss cross sections obtained by adding the LPA antiscreening contribution and each one of the three screening curves displayed in (a); squares, measurements of Sant'Anna *et al.* [50].

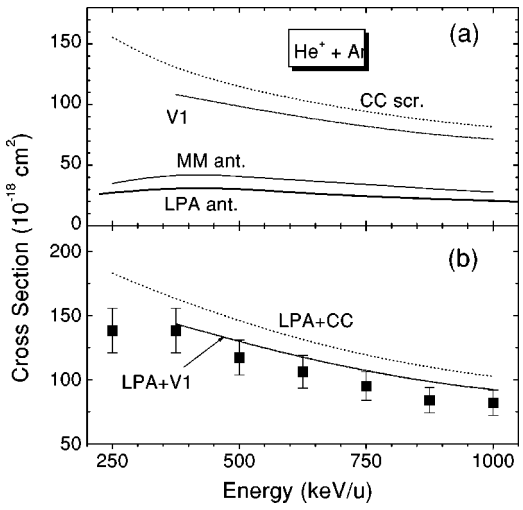

FIG. 8. Projectile-electron-loss cross sections for He^+ impinging on Ar. Notation: (a) thick solid line, presents LPA results; thin solid line, antiscreening calculations following the procedure of Montenegro and Meyerhof [3,7]; dotted line, Grande *et al.* screening curve [1]; dash-dotted line, nonperturbative screening of Voitkiv *et al.* [49]; (b) theoretical curves of the total electron-loss cross sections obtained by adding the LPA antiscreening contribution and each one of the screening curves displayed in (a); squares, measurements of Sant'Anna *et al.* [50].

For the comparison with the experimental data of total electron loss we need to add the screening contribution.

The results obtained are displayed in Figs. 6–9. In the upper figures (a) we show the LPA antiscreening curves together with the antiscreening results following the procedure of Montenegro and Meyerhof [1,3,7] and different screening curves [1,3,49]. In the bottom figures (b) we display total cross sections and the experimental data available.

The comparison between the antiscreening curves shows that the LPA calculations are always below the Montenegro antiscreening ones [1,3,7] [see part (a) of Figs. 6–9]. The difference between these antiscreening results grows up with the number of target electrons, i.e., from He to Kr targets, and diminishes with higher impact energies. However, the LPA is expected to be better for Kr than for He, just because in Kr atoms we have more electrons less bound which are more liable to be represented as a free-electron gas than the two He electrons. On the other hand, the inclusion of the screening of the projectile potential by the target electrons is coherent with a reduction of the cross sections [41]. This screening effect is present in the LPA which works within the dielectric formalism and not in the binary collision one. And this effect grows up with the number of target electrons and diminishes with higher impact velocities, just as the difference between the antiscreening curves.

In part (a) of Figs. 6–9, we also include the screening curves of Grande *et al.* [1] by using the coupled-channel method, the sudden perturbation curves of Voitkiv *et al.* [49], and the screening curves corrected by the factor $1-P_{ion}$ to take into account the probability of target ionization by the screened projectile [3]. In the case of He target, Fig. 6(a), the comparison of the screening and antiscreening mechanisms shows that they tend to equipartition, as already found by Montenegro *et al.* [10].

The difference between the three screening curves and the fact that the screening contribution is the main one for heavy targets [1,49] makes difficult the evaluation of the antiscreening LPA results by comparing them with the total electron loss data.

The total electron-loss cross sections are displayed in part (b) of Figs. 6–9. We add the antiscreening results obtained with the LPA and the different theoretical screening calculations [1,3,49]. For He target, which is more sensitive to the

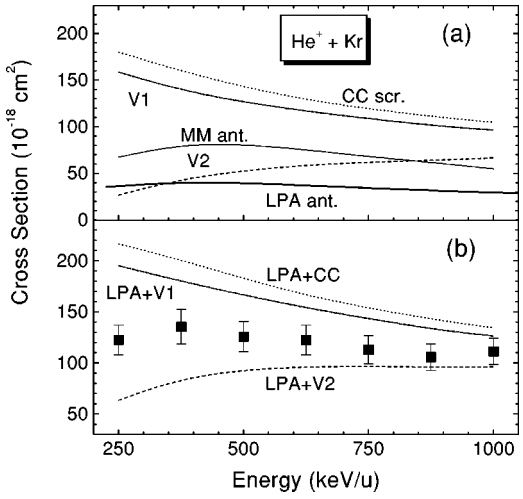

FIG. 9. The same as in Fig. 7.

antiscreening contribution, we find good accord with the experimental data of Sant'Anna *et al.* [50]. For Ne, Ar, and Kr targets, the discrepancy between the theoretical screening results is more significative than the antiscreening contribution. This discrepancy appears in the total electron-loss curves too.

IV. CONCLUSIONS

The LPA represents a good high velocity estimation of the whole inelastic processes that take place in the target. On the other hand, the model is very simple, and the calculations are much faster than the usual atomic antiscreening ones or the CDW-EIS calculations. The range of validity is limited to the perturbative regime and to those impinging velocities higher than the velocity of the target electrons. This limitation is related to the description of the bound electrons as a free-electron gas of inhomogeneous density. Nevertheless, the comparison with the experiments indicates that this range of validity can be extended. The extension of the dielectric formalism, developed originally for solids, to gases is in accord with a previous work where the binary collision and the dielectric formalisms are compared. The employment of the dielectric formalism applied to gases introduces the screening of target electrons over the ion potential.

The good agreement with the experimental data and the simplicity of the local-density approximation make it an efficient method for describing the inelastic processes of gaseous target electrons. It is designed to be useful for targets with large atomic number. In these cases, the number of possible final states to be considered by the traditional atomic methods makes it a tough task to be tackled. On the contrary, the more electrons the target has, the better the local plasma approximation is expected to be.

ACKNOWLEDGMENTS

We thank E. C. Montenegro and P. L. Grande for useful discussions and comments on the subject. This work was partially supported by the Agencia Nacional de Investigacion Cientifica y Tecnologica of Argentina, Grant Nos. PICT 03-03579 and PICT99 03-06249, and by the Universidad de Buenos Aires, Grant No. UBACyT X044.

[1] P.L. Grande, G. Schwiwietz, G.M. Sigaud, and E.C. Montenegro, Phys. Rev. A **54**, 2983 (1996).
[2] G.M. Sigaud, F.S. Joras, A.C.F. Santos, E.C. Montenegro, M.M. Sant'Anna, and W.S. Melo, Nucl. Instrum. Methods Phys. Res. B **132**, 312 (1997).
[3] A.B. Voitkiv, G.M. Sigaud, and E.C. Montenegro, Phys. Rev. A **59**, 2794 (1999).
[4] T. Kirchner and M. Horbatsch, Phys. Rev. A **63**, 062718 (2001).
[5] J.H. McGuire, N. Stolterfoht, and P.R. Simony, Phys. Rev. A **24**, 97 (1981).
[6] R. Anholt, Phys. Lett. **114A**, 126 (1986).
[7] E.C. Montenegro and W.E. Meyerhof, Phys. Rev. A **43**, 2289 (1991).
[8] E.C. Montenegro and W.E. Meyerhof, Phys. Rev. A **46**, 5506 (1992).
[9] E.C. Montenegro, W.S. Melo, W.E. Meyerhof, and A.G. Pinho, Phys. Rev. Lett. **69**, 3033 (1992).
[10] E.C. Montenegro, W.S. Melo, W.E. Meyerhof, and A.G. Pinho, Phys. Rev. A **48**, 4259 (1993).
[11] D.H. Lee, T.J.M. Zouros, J.M. Sanders, P. Richard, J.M. Anthony, Y.D. Wang, and J.H. McGuire, Phys. Rev. A **46**, 1374 (1992).
[12] E.C. Montenegro and T.J.M. Zouros, Phys. Rev. A **50**, 3186 (1994).
[13] W. Wu, K.L. Wong, R. Ali, C.Y. Chen, C.L. Cocke, V. Frohne, J.P. Giese, M. Raphaelian, B. Walch, R. Dörner, V. Mergel, H. Schmidt-Böcking, and W.E. Meyerhof, Phys. Rev. Lett. **72**, 3170 (1994).
[14] R. Dörner, V. Mergel, R. Ali, U. Buck, C.L. Cocke, K. Froschaauer, O. Jagutzki, S. Lencinas, W.E. Meyerhof, S. Nüttgens, R.E. Olson, H. Schmidt-Böcking, L. Spielberger, K. Tökesi, J. Ullrich, M. Unverzagt, and W. Wu, Phys. Rev. Lett. **72**, 3166 (1994).
[15] H.P. Hulskotter *et al.*, Phys. Rev. A **44**, 1712 (1991).
[16] C.C. Montanari, J.E. Miraglia, and N.R. Arista, Phys. Rev. A **62**, 052902 (2000).
[17] D.G. Arbo and J.E. Miraglia, Phys. Rev. A **58**, 2970 (1998).
[18] C.C. Montanari, J.E. Miraglia, and N.R. Arista, Phys. Rev. A **66**, 042902 (2002).
[19] J. Linhard and M. Scharff, K. Dan. Vidensk. Selsk. Mat. Fys. Medd. **27**, 15 (1953).
[20] J.D. Fuhr, V.H. Ponce, F.J. Garcia de Abajo, and P.M. Echenique, Phys. Rev. B **57**, 9329 (1998).
[21] J. Calera-Rubio, A. Gras-Marti, and N.R. Arista, Nucl. Instrum. Methods Phys. Res. B **93**, 137 (1994).
[22] A. Sarasola, J.D. Fuhr, V.H. Ponce, and A. Arnau, Nucl. Instrum. Methods Phys. Res. B **182**, 67 (2001).
[23] P.M. Echeniquee, F. Flores, and R.H. Ritchie, Solid State Phys. **43**, 229 (1990).
[24] I. Abril, R. Garcia-Molina, C.D. Denton, F.J. Perez-Perez, and N.R. Arista, Phys. Rev. A **58**, 357 (1998).
[25] E. Clementi and C. Roetti, At. Data Nucl. Data Tables **14**, 177 (1974).
[26] C.J. Joachain, *Quantum Collision Theory* (North-Holland, Amsterdam, 1975), Vol. 1.
[27] S.T. Manson, Phys. Rev. A **5**, 668 (1972).
[28] D.H. Madison, Phys. Rev. A **8**, 2449 (1973).
[29] S.T. Manson, L.H. Toburen, D.H. Madison, and N. Stolterfoht, Phys. Rev. A **12**, 60 (1975).
[30] A. Salin, J. Phys. B **22**, 3901 (1989).
[31] J. Linhard, K. Dan. Vidensk. Selsk. Mat. Fys. Medd. **28**, 8 (1954).
[32] E.C. Montenegro, A.C.F. Santos, W.S. Melo, M.M. Sant'Anna, and G.M. Sigaud, Phys. Rev. Lett. **88**, 013201 (2002).
[33] U. Kadhane, C.C. Montanari, and L.C. Tribedi, Phys. Rev. A **67**, 032703 (2003).

[34] L. Gulyás, P. Fainstein, and A. Salin, J. Phys. B **28**, 245 (1995).
[35] M.E. Rudd, Y.K. Kim, D.H. Madison, and Gallagher, Rev. Mod. Phys. **57**, 965 (1985).
[36] N. Stolterfoht, D. Scheneider, and P. Ziem, Phys. Rev. A **10**, 81 (1974).
[37] M.E. Rudd, Phys. Rev. A **10**, 518 (1974).
[38] W.M. Ariyasinghe, H.T. Awuku, and D. Powers, Phys. Rev. A **42**, 3819 (1990).
[39] B.B. Dhal, L.C. Triberdi, U. Tiwari, K.V. Thulasiram, P.N. Tandom, T.G. Lee, C.D. Lin, and L. Gulyás, Phys. Rev. A **62**, 022714 (2000).
[40] T. Kirchner, H.J. Lüdde, M. Horbatsch, and R.M. Dreizler, Phys. Rev. A **61**, 052710 (2000).
[41] T. Kirchner, M. Horbatsch, H.J. Lüdde, and R.M. Dreizler, Phys. Rev. A **62**, 042704 (2000).
[42] W.R. Thompson, M.B. Shah, J. Geddes, and H.B. Gilbody, J. Phys. B **30**, L207 (1997).
[43] W.R. Thompson, M.B. Shah, and H.B. Gilbody, J. Phys. B **28**, 1321 (1995).
[44] D.K. Brice, Phys. Rev. A **6**, 1791 (1972); **19**, 1367 (1979); Appl. Phys. Lett. **29**, 10 (1976).
[45] S. Cruz, Radiat. Eff. **86**, 159 (1986), and references therein.
[46] R. Cabrera-Trujillo, J.R. Sabin, Y. Ohrn, and E. Deumens, Phys. Rev. Lett. **84**, 5300 (2000).
[47] S.K. Allison, J. Cuevas, and M. García-Muñoz, Phys. Rev. **127**, 792 (1962).
[48] H.K. Reynolds, D.N. Dunbar, W.A. Wenzel, and W. Whaling, Phys. Rev. **92**, 742 (1953).
[49] A.B. Voitkiv, N. Grün, and W. Scheid, J. Phys. B **33**, 3439 (2000).
[50] M. M. SantAnna, W.S. Melo, A.C.F. Santos, G.M. Sigaud, and E.C. Montenegro, Nucl. Instrum. Methods Phys. Res. B **99**, 46 (1995).